

# Highly Efficient Green Organic Light-Emitting Diodes Containing Luminescent Three-Coordinate Copper(I) Complexes

Masashi Hashimoto,<sup>†,‡</sup> Satoshi Igawa,<sup>†,‡</sup> Masataka Yashima,<sup>†,‡</sup> Isao Kawata,<sup>†,§</sup> Mikio Hoshino,<sup>‡</sup> and Masahisa Osawa<sup>\*,†</sup>

<sup>†</sup>Luminescent Materials Laboratory, RIKEN (The Institute of Physical & Chemical Research), Hirosawa 2-1, Wako-Shi 351-0198, Japan

<sup>‡</sup>Device Technology Development Headquarters and <sup>§</sup>Analysis Technology Center, Canon Incorporated, Ohta-ku, Tokyo 146-8501, Japan

 Supporting Information

**ABSTRACT:** A series of highly emissive three-coordinate copper(I) complexes, (dtpb)Cu<sup>I</sup>X [X = Cl (**1**), Br (**2**), I (**3**); dtpb = 1,2-bis(*o*-ditolylphosphino)benzene], were synthesized and investigated in prototype organic light-emitting diodes (OLEDs). **1–3** showed excellent photoluminescent performance in both degassed dichloromethane solutions [quantum yield ( $\Phi$ ) = 0.43–0.60; lifetime ( $\tau$ ) = 4.9–6.5  $\mu$ s] and amorphous films ( $\Phi$  = 0.57–0.71;  $\tau$  = 3.2–6.1  $\mu$ s). Conventional OLEDs containing **2** in the emitting layer exhibited bright green luminescence with a current efficiency of 65.3 cd/A and a maximum external quantum efficiency of 21.3%.

Much effort has been devoted to improving the external quantum efficiency (EQE, photons per electron) of organic light-emitting diodes (OLEDs). OLEDs doped with phosphorescent metal complexes, such as cyclometalated iridium(III) complexes, can exhibit high EQEs of >20%.<sup>1</sup> This value is much higher than the theoretical limit of 5% for fluorescent OLEDs. Over the past two decades, phosphorescent and delayed-fluorescent tetrahedral copper(I) complexes containing two bidentate ligands (bisimine and/or bisphosphine ligands) have received increasing attention as dopants because of the low cost and stable supply of copper metal.<sup>2,4b</sup> However, tetrahedral copper(I) complexes tend to display weak emission because of excited-state distortion, which accelerates non-radiative decay of the emissive excited state. According to earlier studies,<sup>3</sup> the use of sterically congested ligands affords a rigid environment around the copper center in the complexes, leading to effective suppression of the nonradiative processes caused by (i) Jahn–Teller distortion of emissive excited states with metal-to-ligand charge transfer (MLCT) character, (ii) ligand dissociation in the excited state, and (iii) solvent-induced exciplex formation. Recently, Harkins and Peters reported {(PNP)Cu<sup>I</sup>}<sub>2</sub>, a highly emissive bimetallic copper(I) complex wherein two tetrahedral Cu<sup>I</sup> units are bridged by the amido groups of the rigid, bulky PNP ligand [PNP<sup>−</sup> = bis(2-diisobutylphosphinophenyl)amido].<sup>4a</sup> An optimized EQE of 16.1% was achieved for vapor-deposited OLEDs containing the analogous complex {(PNP-<sup>t</sup>Bu)Cu<sup>I</sup>}<sub>2</sub> [PNP-<sup>t</sup>Bu<sup>−</sup> = bis(2-diisobutylphosphino-4-*tert*-butylphenyl)amido].<sup>4b</sup>

Herein we describe the synthesis and photophysical properties of (dtpb)Cu<sup>I</sup>X [X = Cl (**1**), Br (**2**), I(**3**)], a simple three-coordinate

copper(I) system containing a chelating bisphosphine ligand [dtpb = 1,2-bis(*o*-ditolylphosphino)benzene], and the use of these complexes as dopants in OLEDs. A vapor-deposited OLED doped with **2** exhibited a maximum EQE of 21.3%.

The bidentate bisphosphine ligand dtpb was synthesized by addition of 2-methylphenylmagnesium bromide to 1,2-bis-(dichlorophosphino)benzene in THF at 0 °C under argon.<sup>5</sup> Complexes **1–3** were prepared in 75–95% yield by mixing a suspension of CuX (X = Cl for **1**, Br for **2**, I for **3**) in dichloromethane with 1 equiv of dtpb. Single crystals of **1–3** suitable for X-ray analysis were obtained by layering of Et<sub>2</sub>O on the surface of solutions of the complexes in CHCl<sub>3</sub> (for **1**) or CH<sub>2</sub>Cl<sub>2</sub> (for **2** and **3**).

Single-crystal X-ray diffraction studies of **1–3** revealed monomeric three-coordinate structures. The molecular structure of **2** is shown in Figure 1 as an example. The coordination geometries of the copper centers in **1–3** are trigonal-planar; the sum of the angles around the Cu(I) center are 359.66, 359.37, and 359.43°, respectively. The *o*-methyl groups of dtpb are required for the formation of three-coordinate complexes because 1,2-bis-(diphenylphosphino)benzene (dppb), which lacks methyl groups, forms only the halogen-bridged binuclear copper complexes [Cu( $\mu$ -X)dppb]<sub>2</sub> with CuX.<sup>2h</sup> This is probably because the Cu<sub>2</sub>X<sub>2</sub> diamond core in [Cu( $\mu$ -X)dtpb]<sub>2</sub> would be highly unstable as a result of steric hindrance of the *o*-methyl groups located on the sides of the metal centers, causing the unusual monomeric three-coordinate structures to be produced. The introduction of a bulky substituent on the ligand appears to be necessary to produce three-coordinate copper complexes. Recently, emissive three-coordinate copper(I) complexes with bulky anions (monodentate amide ligands or N-heterocyclic carbene ligands with bulky substituents) have been reported.<sup>6</sup> The Cu–P distances (2.2442–2.2768 Å) in **1–3** are almost equal to those in [Cu( $\mu$ -X)dppb]<sub>2</sub>, indicating that the chelating ability of dtpb is similar to that of dppb.

The absorption and emission spectra of dtpb and copper(I) complexes **1–3** are shown in Figure 2. The absorption spectrum of dtpb exhibits a broad, intense band at 289 nm ( $\epsilon$  = 1.92 × 10<sup>4</sup> M<sup>−1</sup> cm<sup>−1</sup>), which is characteristic of an arylphosphine compound. This band is assigned to a mixed transition of n →  $\pi^*$  and  $\pi$  →  $\pi^*$ ; the former is the transition of an electron from the lone-pair orbital on phosphorus to an empty antibonding  $\pi^*$  orbital on

Received: March 31, 2011

Published: May 17, 2011

a phenyl ring, and the latter are transitions localized on a tolyl or phenylene ring or those from a tolyl ring to a phenylene ring.<sup>7</sup> Complexes 1–3 show more complicated spectra than dtpb; the spectra possess a broad band with a maximum at 300–303 nm [ $\epsilon = (1.13–1.28) \times 10^4 \text{ M}^{-1} \text{ cm}^{-1}$ ] and a shoulder at  $\sim 370$  nm. These two absorption bands are assigned to a mixed transition of  $\sigma \rightarrow \pi^*$  and  $\pi \rightarrow \pi^*$  and an  $X \rightarrow \pi^*$  (dtpb) transition ( $X = \text{Cl}, \text{Br}, \text{I}$ ), respectively, analogous to those in related tetrahedral copper complexes.<sup>2h,8</sup>

The photoluminescence properties of complexes 1–3 are presented in Table 1. While solutions of dtpb do not luminesce at 293 K, complexes 1–3 emit intense green phosphorescence in degassed  $\text{CH}_2\text{Cl}_2$  solutions at 293 K with phosphorescence quantum yields ( $\Phi$ ) of 0.43, 0.47, and 0.60, respectively. The phosphorescence lifetimes ( $\tau$ ) of the three complexes were measured after laser excitation at 355 nm; the phosphorescence decay profiles are illustrated in the inset of Figure 2, from which  $\tau$  values of 4.9, 5.4, and 6.5  $\mu\text{s}$  were calculated for 1–3, respectively. The emission maxima ( $\lambda_{\text{max}}$ ) of 1–3 show the order  $3 < 2 < 1$ , suggesting that  $\lambda_{\text{max}}$  is affected by the ligand-field strength ( $\text{I}^- < \text{Br}^- < \text{Cl}^-$ ). Presumably the electronic nature of the triplet

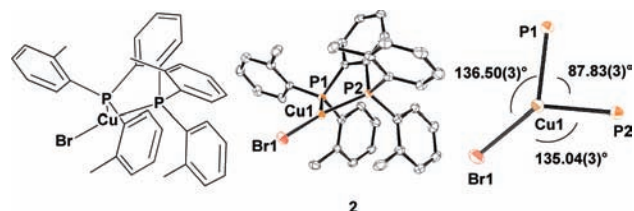


**Figure 1.** (left) Molecular structure of 2. (center) ORTEP view of 2. Thermal ellipsoids are drawn at the 50% probability level, and H atoms have been omitted for clarity. (right) Core structure of 2.

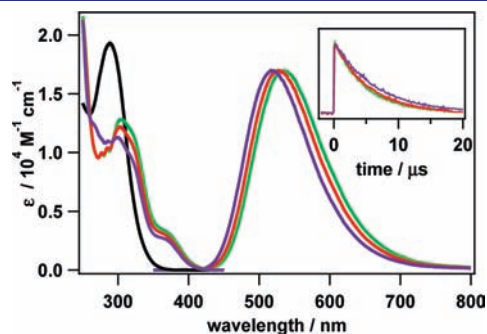


**Figure 2.** Absorption and corrected emission spectra of dtpb (black), 1 (green), 2 (red), and 3 (purple). The inset shows the observed decay profiles of the phosphorescence from 1–3 after excitation at 355 nm at 293 K.

excited state of 1–3 is influenced to some extent by  $X^- \rightarrow \pi^*$  (dtpb) charge-transfer transitions.

The electrochemical properties of these complexes were investigated by cyclic voltammetry (CV). Irreversible oxidation waves at 407, 432, 468, and 443 mV vs  $\text{Fc}^+/\text{Fc}$  for dtpb and 1–3, respectively, were observed. This result suggests that orbitals of the Cu(I) atom and those of the halogen atom partially contribute to the highest occupied molecular orbitals (HOMOs) of 1–3.

Natural transition orbital (NTO) analysis revealed that these transitions can be described as single hole/electron pairs and reproduce over 95% of the change in electron density upon excitation. The hole (approximately HOMO) and electron [approximately the lowest unoccupied molecular orbital (LUMO)] distributions for the lowest triplet state of 2 at the  $T_1$  optimized geometry are shown in Figure 3A. The hole distribution of 2 is essentially halogen-based but also includes the orbitals with  $\sigma$  character between the Cu(I) and P atoms; the contributions from the Br, Cu, and P atoms to the hole distribution are 16, 28, and 31%, respectively. The electron distribution is largely confined to the *o*-phenylene group in the dtpb ligand. Excited-state calculations carried out for 1–3 indicated that phosphorescence results from the transitions  $(\sigma + X) \rightarrow \pi^*$ . Another notable feature of 2 is that there is little structural change between the ground and excited states. Furthermore, the singlet–triplet energy gaps are very small (2.63–4.51 kcal/mol) in all of the optimized structures, as shown in Figure 3B.

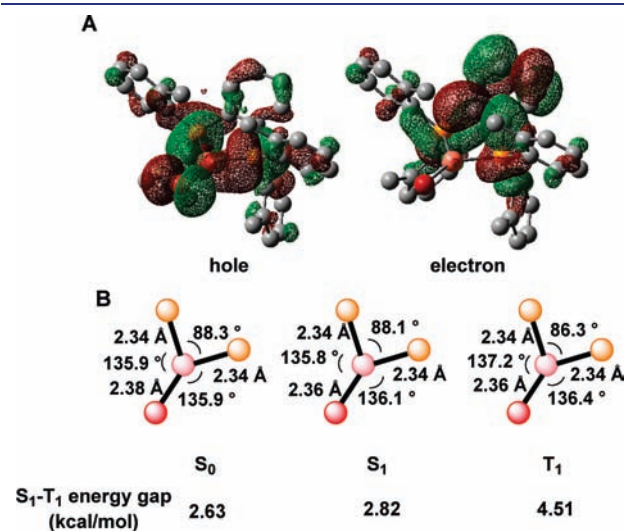


**Figure 3.** (A) NTO pairs for the lowest triplet excited state of 2 at the  $T_1$  optimized geometry. (B) Optimized core structures of 2 in the ground state ( $S_0$ ) and the singlet ( $S_1$ ) and triplet ( $T_1$ ) excited states and the energy gap between the  $S_1$  and  $T_1$  levels in each optimized structure.

**Table 1. Photophysical Data for 1–3 at 293 K**

complex	emission in $\text{CH}_2\text{Cl}_2$			emission in mCP (containing 10% complexes)		
	$\lambda_{\text{max}}$ (nm) <sup>a</sup>	$\Phi_{\text{PL}}$ <sup>b</sup>	$\tau$ ( $\mu\text{s}$ ) <sup>c</sup>	$\lambda_{\text{max}}$ (nm)	$\Phi_{\text{PL}}$	$\tau$ ( $\mu\text{s}$ ) <sup>d</sup>
1	534	0.43	4.9	520	0.68	6.1 (4.6)
2	527	0.47	5.4	514	0.71	5.5 (3.9)
3	517	0.60	6.5	504	0.57	3.2 (1.4)

<sup>a</sup> PL maximum. <sup>b</sup> Absolute PL quantum yield. <sup>c</sup> PL lifetime. <sup>d</sup> PL lifetime is composed of two components. The faster component is shown in parentheses.

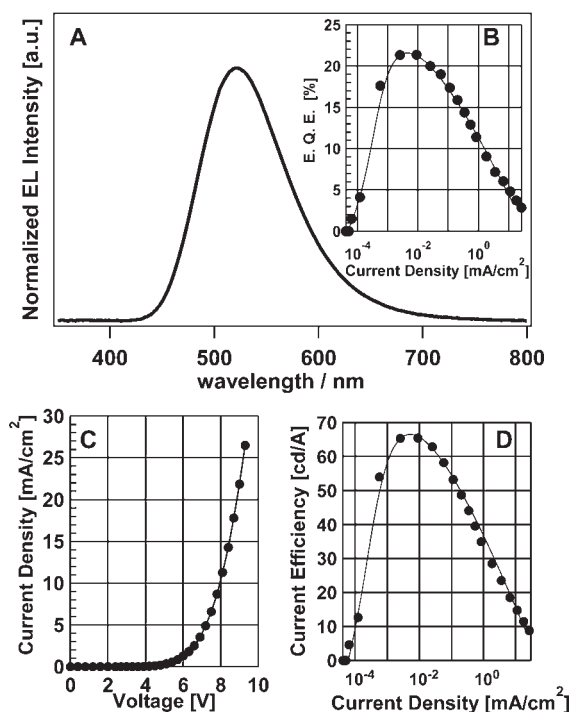


**Figure 4.** Properties of an OLED containing **2** as a dopant: (A) EL spectrum; (B) dependence of EQE on current density; (C)  $I$ – $V$  characteristics; (D) dependence of current efficiency on current density.

Barakat observed Jahn–Teller distortion from Y- to T-shaped geometry in the triplet excited state of trigonal planar Au(I) complexes containing three monophosphine ligands  $[\text{Au}(\text{PR}_3)_3]^+$ .<sup>9</sup> Our calculations predicted that the Cu(I) complex  $[\text{Cu}(\text{PMe}_3)_3]^+$  with a structure similar to that of  $[\text{Au}(\text{PMe}_3)_3]^+$  should undergo comparable distortion in the excited state.<sup>10</sup> The contribution of MLCT character to the excited state is necessary for excited-state distortion in the Au(I) and Cu(I) complexes. Although there is 28% MLCT character in the triplet excited state of complex **2**, the distortion is markedly small, as shown in Figure 3. Presumably the bisphosphine ligand largely prevents Jahn–Teller distortion in the three-coordinate Cu(I) complexes. The small distortion of the excited states of **2** is assumed to reduce the rate of nonradiative decay, leading to a high  $\Phi$ .

As described above, complexes **1**–**3** exhibit strong phosphorescence in dichloromethane solution. Prior to preparation of OLEDs, the phosphorescence from evaporated amorphous films containing **1**–**3** was investigated using layers of 1,3-bis(carbazol-9-yl)benzene (mCP) doped with 10% **1**–**3** with a thickness of 50 nm deposited onto a quartz plate. The amorphous films exhibited  $\Phi$  values of 0.57–0.71 and  $\tau$  values of 3.2–6.1  $\mu\text{s}$  (Table 1). On the basis of the PL data for the doped samples, complex **2** was selected for use as a dopant in an OLED. Except for **2**, the materials used to make the device are commercially available. A bottom-emitting device with a three-layer structure of ITO (110 nm)/TAPC (30 nm)/mCP + 10% **2** (25 nm)/3TPYMB (50 nm)/LiF (0.5 nm)/Al (100 nm), where TAPC is di-[4-(*N,N*-ditolylamino)phenyl]cyclohexane and 3TPYMB is tris[2,4,6-trimethyl-3-(pyridine-3-yl)phenyl]borane, was fabricated. The electroluminescence (EL) of **2** ( $\lambda_{\text{max}} = 517$  nm) is in good agreement with the PL data, as shown in Figure 4A and Table 1. The current–voltage ( $I$ – $V$ ) characteristics of the device

containing **2** indicate a turn-on voltage of 2.7 V (Figure 4C). A maximum current efficiency of 65.3 cd/A was achieved at 0.01 mA/cm<sup>2</sup>, which corresponds to a maximum EQE of 21.3% (Figure 4B,D). This efficiency is comparable to that of cyclometalated iridium(III)-based devices, which currently set the standard for efficiency. The present work suggests that three-coordinate copper(I) complexes are promising EL materials in terms of efficiency and thermal stability. Detailed studies of the photophysics of these three-coordinate copper complexes are in progress.

## ■ ASSOCIATED CONTENT

**S Supporting Information.** X-ray crystallographic data (CIF), synthetic details, time-dependent density functional theory calculations, and a table of experimental data. This material is available free of charge via the Internet at <http://pubs.acs.org>.

## ■ AUTHOR INFORMATION

**Corresponding Author**  
osawa@postman.riken.jp

## ■ ACKNOWLEDGMENT

The authors acknowledge Dr. Daisuke Hashizume for technical assistance with X-ray structural analysis.

## ■ REFERENCES

- (1) (a) Adachi, C.; Baldo, M. A.; Thompson, M. E.; Forrest, S. R. *J. Appl. Phys.* **2001**, *90*, 5048–5051. (b) Tanaka, D.; Agata, Y.; Sasabe, S.; Li, Y.-J.; Su, S.-J.; Takeda, T.; Kido, J. *Jpn. J. Appl. Phys.* **2007**, *46*, L10–L12. (c) Tanaka, D.; Agata, Y.; Takeda, T.; Watanabe, S.; Kido, J. *Jpn. J. Appl. Phys.* **2007**, *46*, L117–L119. (d) Kondakova, M. E.; Pawlik, T. D.; Young, R. H.; Giesen, D. J.; Kondakov, D. Y.; Brown, C. T.; Deaton, J. C.; Lenhard, J. R.; Klubek, K. P. *J. Appl. Phys.* **2008**, *104*, No. 094501. (e) Chopra, N.; Lee, J.; Zheng, Y.; Eom, S.-H.; Xue, J.; So, F. *Appl. Phys. Lett.* **2008**, *93*, No. 143307.
- (2) (a) Zhang, Q.; Zhou, Q.; Cheng, Y.; Wang, L.; Ma, D.; Jing, X.; Wang, F. *Adv. Mater.* **2004**, *16*, 432–436. (b) Jia, W. L.; McCormick, T.; Tao, Y.; Lu, J.-P.; Wang, S. *Inorg. Chem.* **2005**, *44*, 5706–5712. (c) Zhang, Q.; Zhou, Q.; Cheng, Y.; Wang, L.; Ma, D.; Jing, X.; Wang, F. *Adv. Funct. Mater.* **2006**, *16*, 1203–1208. (d) Amaroli, N.; Accorsi, G.; Holler, M.; Moudam, O.; Nierengarten, J.-F.; Zhou, Z.; Wegh, R. T.; Welter, R. *Adv. Mater.* **2006**, *18*, 1313–1316. (e) Su, Z.; Che, G.; Li, W.; Su, W.; Li, M.; Chu, B.; Li, B.; Zhang, Z.; Hu, Z. *Appl. Phys. Lett.* **2006**, *88*, No. 213508. (f) Che, G.; Su, Z.; Li, W.; Chu, B.; Li, M.; Hu, Z.; Zhang, Z. *Appl. Phys. Lett.* **2006**, *89*, No. 103511. (g) Zhang, Q.; Ding, J.; Cheng, Y.; Wang, L.; Xie, Z.; Jing, X.; Wang, F. *Adv. Funct. Mater.* **2007**, *17*, 2983–2990. (h) Tsuboyama, A.; Kuge, K.; Furugori, M.; Okada, S.; Hoshino, M.; Ueno, K. *Inorg. Chem.* **2007**, *46*, 1992–2001. (i) Moudam, O.; Kaeser, A.; Delavaux-Nicot, B.; Duhayon, C.; Holler, M.; Accorsi, G.; Armaroli, N.; Seguy, I.; Navarro, J.; Destruel, P.; Nierengarten, J.-F. *Chem. Commun.* **2007**, 3077–3079. (j) Si, Z.; Li, J.; Li, B.; Liu, S.; Li, W. *J. Lumin.* **2009**, *129*, 181–186. (k) Zhang, L.; Li, B.; Su, Z. *J. Phys. Chem. C* **2009**, *113*, 13968–13973.
- (3) (a) McMillin, D. R.; McNett, K. M. *Chem. Rev.* **1998**, *98*, 1201–1220. (b) Ford, P. C.; Cariati, E.; Bourassa, J. *Chem. Rev.* **1999**, *99*, 3625–3647. (c) Armaroli, N.; Accorsi, G.; Cardinali, F.; Listorti, A. *Top. Curr. Chem.* **2007**, *280*, 69–115. (d) Felder, D.; Nierengarten, J.-F.; Barigelletti, F.; Ventura, B.; Armaroli, N. *J. Am. Chem. Soc.* **2001**, *123*, 6291–6299. (e) Cuttall, D. G.; Kuang, S. M.; Fanwick, P. E.; McMillin, D. R.; Walton, R. A. *J. Am. Chem. Soc.* **2002**, *124*, 6–7. (f) Kuang, S. M.; Cuttall, D. G.; McMillin, D. R.; Fanwick,

P. E.; Walton, R. A. *Inorg. Chem.* **2002**, *41*, 3313–3322. (g) Kalsani, V.; Schmittl, M.; Listorti, A.; Accorsi, G.; Armaroli, N. *Inorg. Chem.* **2006**, *45*, 2061–2067. (h) Iwamura, M.; Takeuchi, S.; Tahara, T. *J. Am. Chem. Soc.* **2007**, *129*, 5248–5256.

(4) (a) Harkins, S. B.; Peters, J. C. *J. Am. Chem. Soc.* **2005**, *127*, 2030–2031. (b) Deaton, J. C.; Switatski, S. C.; Kondakov, D. Y.; Young, R. H.; Pawlik, T. D.; Giesen, D. J.; Harkins, S. B.; Miller, A. J. M.; Mickenberg, S. F.; Peters, J. C. *J. Am. Chem. Soc.* **2010**, *132*, 9499–9508.

(5) Dennett, J. N. L.; Gillon, A. L.; Heslop, K.; Hyett, D. J.; Fleming, J. S.; Lloyd-Jones, C. E.; Orpen, A. G.; Pringle, P. G.; Wass, D. F.; Scutt, J. N.; Weatherhead, R. H. *Organometallics* **2004**, *23*, 6077–6079.

(6) (a) Lotito, K. J.; Peters, J. C. *Chem. Commun.* **2010**, *46*, 3690–3692. (b) Krylova, V. A.; Djurovich, P. I.; Whited, M. T.; Thompson, M. E. *Chem. Commun.* **2010**, *46*, 6696–6698.

(7) Fife, D. J.; Morse, K. W.; Moore, W. M. *J. Photochem.* **1984**, *24*, 249–263.

(8) (a) Kotal, C. *Coord. Chem. Rev.* **1990**, *99*, 213–252. (b) Kunkely, H.; Pawlowski, V.; Vogler, A. *Inorg. Chem. Commun.* **2008**, *11*, 1003–1005.

(9) Barakat, K. A.; Cundari, T. R.; Omary, M. A. *J. Am. Chem. Soc.* **2003**, *125*, 14228–14229.

(10) Osawa, M.; Kawata, I. Unpublished work.